Evidence for spin-glass states and Griffiths singularities in $Nd_{0.75}Sr_{1.25}CoO_4$

2006 J. Phys.: Condens. Matter 18 7135

(http://iopscience.iop.org/0953-8984/18/31/008)

INSTITUTE OF PHYSICS PUBLISHING JOURNAL OF PHYSICS: CONDENSED MATTER

J. Phys.: Condens. Matter **18** (2006) 7135–7144 doi:10.1088/0953-8984/18/31/008

Evidence for spin-glass states and Griffiths singularities in $Nd_{0.75}Sr_{1.25}CoO_4$

Shengli Huang, Keqing Ruan[1], Zhangming Lv, Huiyan Wu, Zongqiang Pang, Liezhao Cao and Xiaoguang Li

Structure Research Laboratory and Department of Physics, University of Science and Technology of China, Hefei, Anhui 230026, People's Republic of China

E-mail: kqruan@ustc.edu.cn

Received 13 March 2006, in final form 22 May 2006
Published 21 July 2006
Online at stacks.iop.org/JPhysCM/18/7135

Abstract

The magnetic properties of $Nd_{0.75}Sr_{1.25}CoO_4$ have been investigated by means of dc magnetization, ac susceptibility and electron spin resonance measurements. The specimen presented a deviation from the Curie–Weiss law at $T_G \sim 230$ K, ferromagnetic behaviour below $T_C \sim 179$ K, and a cusp structure at $T_{SG} \sim 18$ K in dc magnetization. The cusp was confirmed to be due to the existence of spin-glass states, and the deviation was argued to be a Griffiths singularity. Comparing the magnetic properties of the analogous layered cobalt oxides, the anomalous magnetic features of the specimen were attributed to the introduction of rare-earth ions, Nd^{3+}.

1. Introduction

The 3d transition-metal oxides have attracted much attention due to their unusual physical properties, such as colossal magnetoresistance, superconductivity, spin-glass states, phase separation, orbital and charge orderings. Many theories were provided in order to elucidate their originations. Recently, many intriguing magnetic behaviours in manganese and cobalt oxides were observed in different temperature ranges. At lower temperatures, some magnetic materials such as $Nd_{1-x}Ni_xCoO_3$ [1], $(Nd, La)_{0.5}Sr_{1.5}MnO_4$ [2] and $La_{2-x}Sr_xCoO_4$ [3] behave no longer with ferromagnetic (FM) or antiferromagnetic (AFM) properties but are frozen into spin-glass (SG) states due to the competing FM and AFM interactions with randomness below a temperature $T = T_{SG}$. On the other hand, lots of magnetic materials deviate from the Curie–Weiss law in the paramagnetic range at higher temperatures and behave with lots of interesting singularities. For example, in $LaSr_2Mn_2O_7$ [4], $La_{1-x}Sr_xMnO_3$ [5] and $Pr_{0.6}Y_{0.1}Sr_{0.3}MnO_3$ [6], the inverse values of their dc susceptibilities present a kink or a sharp downturn at a temperature higher than the Curie temperature (T_C). Griffiths *et al*

[1] Author to whom any correspondence should be addressed.

[7, 8] have considered similar phenomena in diluted ferromagnets and proposed a model to interpret it. According to the model, the magnetic materials would be a quenched disordered system in which FM clusters distribute randomly in the paramagnetic (PM) background when the temperature decreases to a critical point. Such a system would present many unusual behaviours in susceptibility, magnetoresistivity, heat capacity, thermopower, etc, above T_C [4, 9–12]. Thus, the critical temperature point is called the Griffiths temperature, T_G, and the temperature range $T_C \leqslant T \leqslant T_G$ is termed the Griffiths phase. Experiments on many manganites agreed very well with the model.

In this work, the magnetic properties of polycrystalline $Nd_{0.75}Sr_{1.25}CoO_4$ are discussed in detail, based on the dc magnetization, ac susceptibility, and electron spin resonance (ESR) experiments. The specimen presents an FM property with $T_C \approx 179$ K. Moreover, it displays SG states at $T_{SG} \approx 18$ K and Griffiths singularities below $T_G \approx 230$ K.

2. Experimental details

The polycrystalline $Nd_{0.75}Sr_{1.25}CoO_4$ was prepared by decomposing the nitrate mixture in KNO_3 [13] and annealing in O_2 atmosphere at 750 K for 30 h. The structure and phase purity of the sample were checked by powder x-ray diffraction (XRD) at room temperature. The dc magnetization and ac susceptibility measurements were performed in a superconducting quantum interference device (SQUID) magnetometer. The dc magnetization was measured as a function of field (H) and temperature (T), respectively. The field dependence of the magnetization (M) was carried out at 90 K as well as 210 K. Also, the temperature dependence of the magnetization, including zero-field-cooling (ZFC) $M_{ZFC}(T)$ and field-cooling (FC) $M_{FC}(T)$, was measured from 5 to 300 K in an applied field of 1000 Oe. The in-phase and out-of-phase components of ac susceptibility, $\chi'(T)$ and $\chi''(T)$, were measured from 2 to 40 K in a driving field of 1000 Oe at different frequencies as well as at a frequency of 80 Hz in different driving fields. ESR measurements were carried out using a JES-FA200 spectrometer, operating at 9.067 GHz, with a scanning field of 0–800 mT in the temperature range 110–300 K.

3. Results and discussion

The powder XRD was consistent with a tetragonal K_2NiF_4 structure (space group: $I4/mmm$). The calculated room-temperature lattice parameters are $a = b = 3.76$ Å and $c = 12.39$ Å with $V = 175.24$ Å^3, in good agreement with the results on polycrystalline compound [13–15]. The dc magnetization measurements revealed FM behaviour for $Nd_{0.75}Sr_{1.25}CoO_4$, as shown in figure 1. The $M_{ZFC}(T)$ and $M_{FC}(T)$ combine with each other at high temperatures, but bifurcate at $T_B \approx 160$ K. With decreasing temperature, both show a sharp increase at the Curie temperature ($T_C \approx 179$ K) followed by a subsequent decrease in $M_{ZFC}(T)$. It is noteworthy that both show a peak at $T_{max} \approx 72$ K and a cusp structure at $T_{SG} \approx 18$ K, as indicated by arrows in figure 1. Moreover, the magnetization above T_C does not follow the Cure–Weiss law over the whole temperature range. It increases smoothly at higher temperatures and shows an augmentation abruptly at $T_G \approx 230$ K. The magnetic anomaly is more obvious in the inverse susceptibility and its derivative as a function of temperature, plotted in figure 2. The χ^{-1} data above T_G can be fitted well to the Curie–Weiss law, indicating a typical feature for paramagnetic behaviour. The Weiss temperature Θ and effective magnetic moment μ_{eff} calculated from the least-squares-fitted straight line are 153.36 K and 3.48 μ_B, respectively. Experiments on powder exhibit similar paramagnetic behaviour from T_G to 400 K, as shown in figure 3, though the temperature point T_G is a little high compared to the ceramic pellet. However, when the

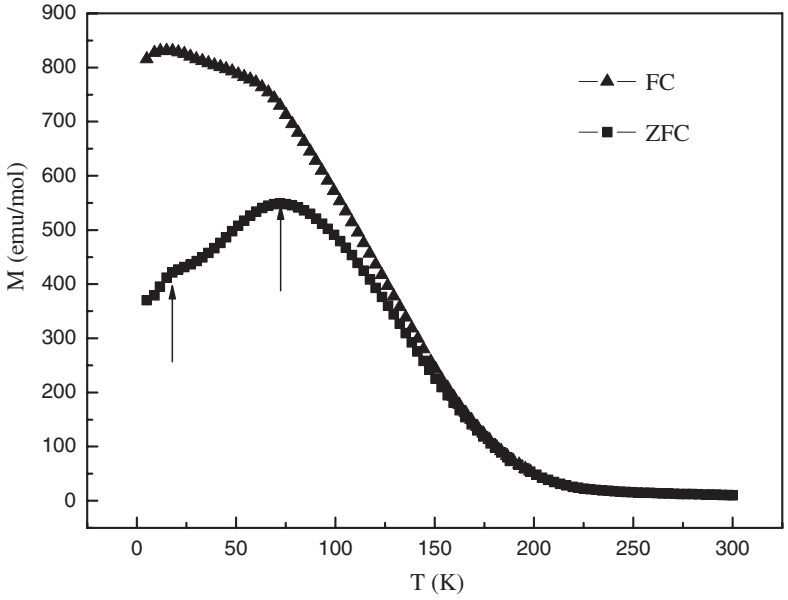

Figure 1. Temperature dependence of the FC and ZFC magnetizations for $Nd_{0.75}Sr_{1.25}CoO_4$.

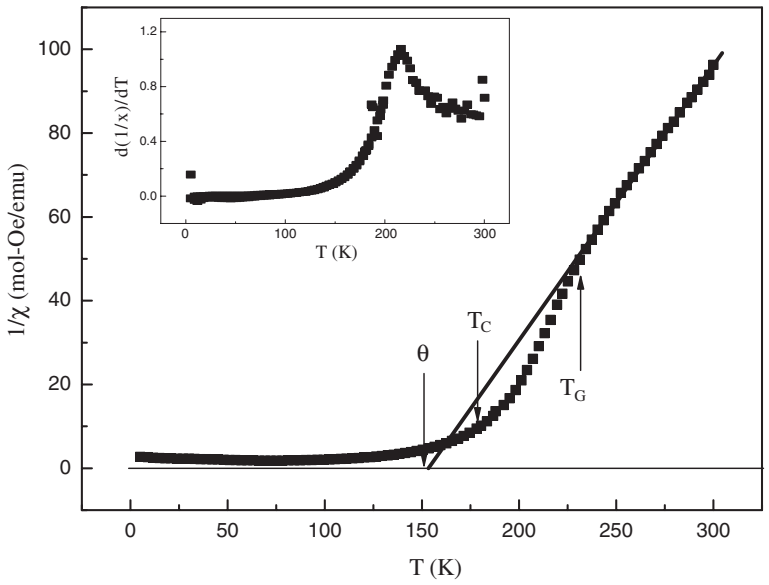

Figure 2. Temperature dependence of the inverse ZFC susceptibility for $Nd_{0.75}Sr_{1.25}CoO_4$. Inset: $d(1/\chi)/dT$ as a function of temperature in $Nd_{0.75}Sr_{1.25}CoO_4$. The solid line is the best fit to the Cure–Weiss law in the paramagnetic range, $T > T_G$.

temperature runs from T_G to T_C, the data show a significant downturn, and a peak emerges in the temperature derivative of χ^{-1}.

Based on the ionic model, the ionic valence and the content of each ion in the specimen is $Nd^{3+}_{0.75}Sr^{2+}_{1.25}Co^{3+}_{0.75}Co^{4+}_{0.25}O^{2-}_4$. As the magnetic moment of Nd^{3+} is hardly influenced by the

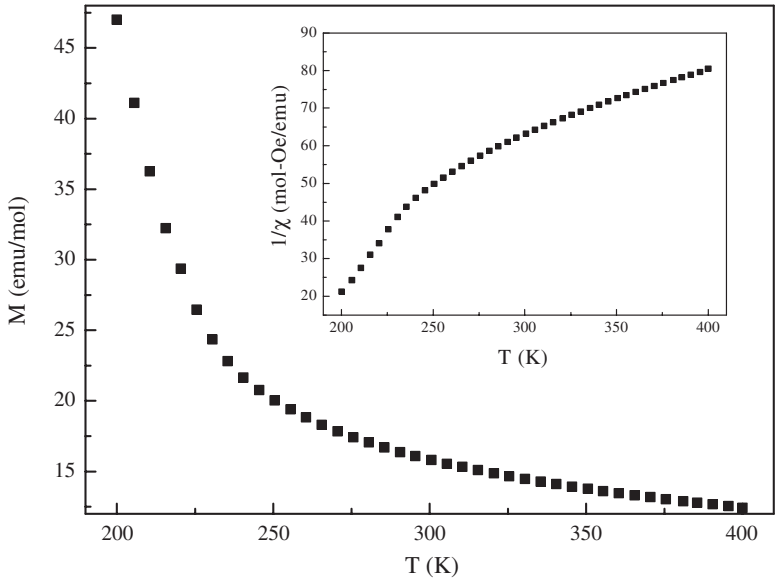

Figure 3. Temperature dependence of the ZFC magnetization for $Nd_{0.75}Sr_{1.25}CoO_4$ powder at 200 K $\leqslant T \leqslant$ 400 K, which was measured in an applied field of 1000 Oe. The inset shows that the susceptibility similarly follows the Curie–Weiss law in the paramagnetic range though the temperature point T_G is a little high compared to the pelleted specimens.

environment [16], the mean magnetic moment of Co ions, Co^{3+} and Co^{4+}, can be estimated roughly by subtracting $\mu_{Nd^{3+}}$ from μ_{eff} in the temperature range above T_G. With Brillouin function, the temperature dependence of the magnetic moment for Nd^{3+} can be calculated, $\mu_{Nd^{3+}} = Jg_J\mu_B B_J(x)$, where J is the angular momentum, g_J is the Lande g factor, μ_B is the Bohr magneton, and $B_J(x)$ is the Brillouin function,

$$B_J(x) = \left(1 + \frac{1}{2J}\right)\coth\left[\left(1 + \frac{1}{2J}\right)x\right] - \left(\frac{1}{2J}\right)\coth\left(\frac{x}{2J}\right),$$

where $x = \frac{Jg_J\mu_0\mu_B H}{k_B T}$. For Nd^{3+}, $J = \frac{9}{2}$ and $g_J = \frac{38}{33}$ (as $S = \frac{3}{2}$, $L = 6$). In the applied field of $H = 1000$ Oe, the variable value $x \ll 0$ when $T \geqslant T_G$, so the Brillouin function can be simplified, $B_J(x) = \frac{x(J+1)}{3J}$. Finally the magnetic moment of a neodymium ion can be obtained, $\mu_{Nd^{3+}} = \frac{\mu_0 g_J^2 J(J+1)\mu_B^2 H}{3k_B T}$. Considering the specimen in a mol quantity, the effective magnetic moment originating from Nd^{3+} is $\mu'_{Nd^{3+}} = 0.75\sqrt{8C}\mu_B = 0.75\sqrt{8\frac{N_A T\mu_{Nd^{3+}}}{H}}\mu_B \approx 0.015\ \mu_B$. The small value implies that the μ_{eff} obtained from susceptibility entirely originates from the cobalt ions. According to references [17, 18], in the parent compound, Sr_2CoO_4, the Co^{4+} is in the intermediate state with $\mu_{eff/Co^{4+}} = 3.87\ \mu_B$, so the magnetic moment of Co^{3+} should be less than 3.48 μ_B if the spin state of Co^{4+} is not changed. As the spin states of Co^{3+} include three configurations in a tetrahedral crystal field—low spin ($t_{2g}^6e_g^0$, $\mu_{eff/Co^{3+}LS} = 0$), intermediate spin ($t_{2g}^5e_g^1$, $\mu_{eff/Co^{3+}IS} = 2.83\ \mu_B$), and high spin ($t_{2g}^4e_g^2$, $\mu_{eff/Co^{3+}HS} = 4.90\ \mu_B$)—the moment value suggests that the Co^{3+} ions in $Nd_{0.75}Sr_{1.25}CoO_4$ are in the intermediate spin state, at least for the higher temperatures above T_G. The result can also be compared with the calculation supposing both Co^{3+} and Co^{4+} ions in the intermediate spin state:

$$2.83 \times 0.75 + 3.87 \times 0.25 = 3.09\ (\mu_B),$$

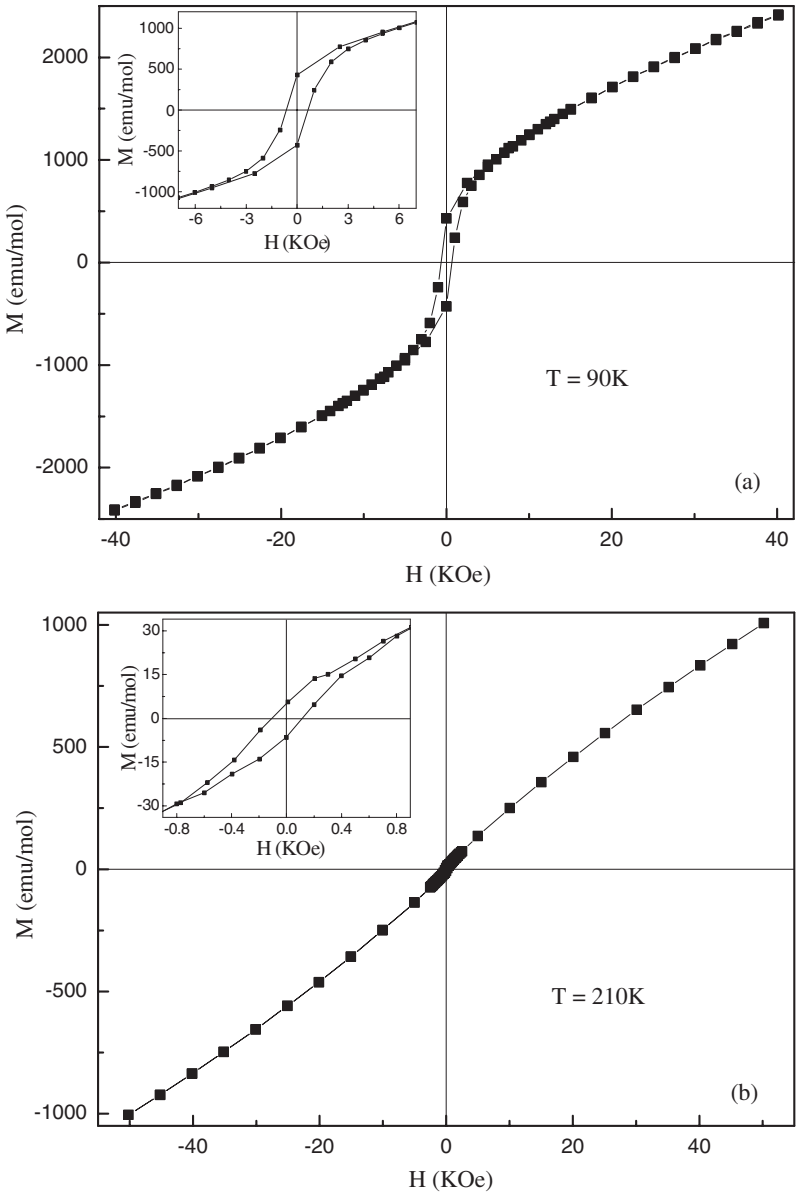

Figure 4. Magnetic hysteresis loops for $Nd_{0.75}Sr_{1.25}CoO_4$ at (a) 90 K and (b) 210 K, respectively. Loops are measured by starting at large positive field, sweeping to negative field, and then returning to positive field. The insets are the enlarged ones at low magnetic field.

which almost equals 3.48 μ_B. The deviation might be ascribed to the oxygen deficiency that increases the number of Co^{4+} ions.

Figure 4 presents the field dependence of magnetization for $Nd_{0.75}Sr_{1.25}CoO_4$ at different temperatures. At 90 K, the curve reveals a ferromagnetic property with a clear magnetic hysteresis. The hysteresis loop shows a relatively large coercive field H_c (660 Oe) and a moderate remnant magnetization M_r (430 emu mol^{-1}), in addition to a component of

magnetization which does not saturate under high magnetic field. Similarly a weak hysteresis is observed in the field dependence of magnetization at 210 K that is near but below T_G, though both H_c and M_r are very small. This feature excludes a superparamagnetic origin of the magnetization, which would result in the disappearance of hysteresis. The magnetization in the high field range (above 9 kOe for $T = 90$ K and 1.5 kOe for $T = 210$ K) can be expressed as $M = M_s + \chi_h H$, where M_s and χ_h stand for the saturation magnetization and high-field susceptibility, respectively. The existence of a finite phase fraction of a non-FM phase, such as the PM or AFM phase, provides an explanation for the non-saturating $M(H)$ behaviour, while the short-range FM clusters could be expected to result in the anomalous hysteresis behaviour just presented in the insets of figure 4. Consulting the great hysteresis loop at 90 K, the peak at T_{max} of ZFC magnetization in figure 1 could just be the result of the magneto-crystalline anisotropy and coercive field for the specimen. That is, with increasing temperature, the magneto-crystalline anisotropy is diminished, and the magnetic moments turn to align to the exoteric field, which induce the increase in magnetization below T_{max}. However, above T_{max} the thermal vibrations bring about spontaneous magnetization that decreases with increasing temperature.

In order to understand the origin of the cusp structure at T_{SG}, ac susceptibility measurements were performed from 2 to 40 K. In figure 5, a characteristic strong peak appears at around T_{SG} in both in-phase and out-of-phase components of ac susceptibility, $\chi'(T)$ and $\chi''(T)$. The peak is frequency dependency and shifts to higher temperatures as the frequency is increased, as shown in figures 5(a) and (b). Furthermore, the peak is depressed when the driving field is intensified; plotted in figures 5(c) and (d). All these results are the typical features of SG [19] and might be explained in terms of SG state, i.e. the frustration of random competing exchange interactions, namely the FM double-exchange interactions between Co^{3+} and Co^{4+} and the AFM super-exchange interactions between like ions. Thus, the cusp structure in figure 1 should be the result of a transition from the FM state to the SG state, and the decreasing magnetization value below T_{SG} might be the introduction of AFM interactions.

The anomaly between T_G and T_C in the dc magnetization curves was also confirmed by ESR measurements, as shown in figure 6. At high temperatures the spectra contain only a PM resonance signal, the A signal, which fits well to the derivative of Dysonian function [20, 21],

$$\frac{dP}{dH} = A\frac{d}{dH}\left[\frac{\Delta H + \alpha(H - H_0)}{4(H - H_0)^2 + \Delta H^2}\right],$$

where A is the area under the curve, ΔH is the line width, H_0 is the centre field and α is the asymmetry parameter representing the ratio of the absorption component to the dispersion component of the response. Figure 7 shows the line fitting at a few typical temperatures. Because the experimental specimen is a polycrystalline ceramic pellet, the Dysonian shape rather than the symmetrical Lorentzian shape may be due to the size of the specimen larger than the electromagnetic skin depth and the local demagnetizing fields. Despite this fact, we can obtain the evolution of the spectra and gain some information from it, as discussed in [21, 22]. With decreasing temperature, the signal broadens gradually and disappears in the end. Concomitantly, another spectrum, the B signal, emerges in the lower resonant field. The B signal intensifies first and then saturates with decreasing temperature. This also rules out the possibility of a superparamagnetic origin of the signal, which would induce a Curie–Weiss-like increase instead of saturation [5]. Because the B signal appears mostly in the FM region, it can be attributed to an FM resonance originating from intergrowth of other parasitic phases undergoing FM transition, just as in $La_{2-x}Sr_{1+x}Mn_2O_7$ [23]. From figure 6, two striking phenomena are noted. First, the resonant field of the PM signal is temperature dependent and moves to a lower field when the temperature decreases, while the FM signal is nearly

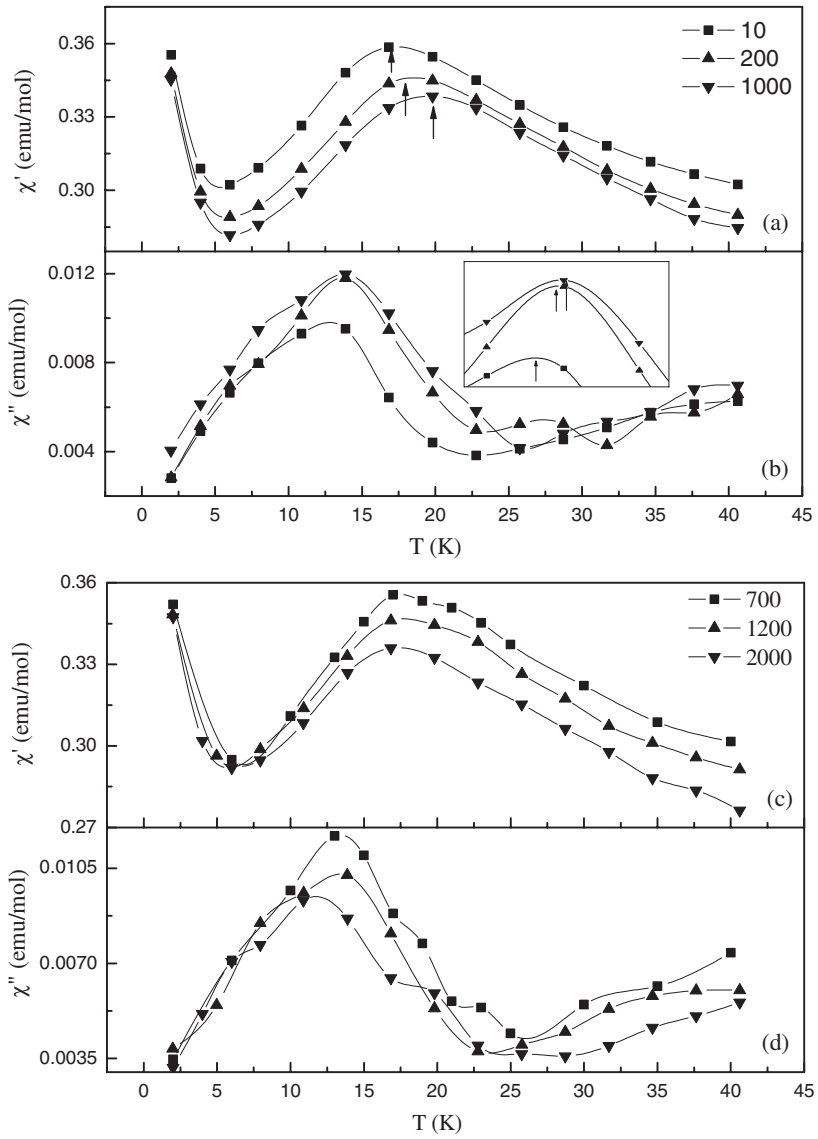

Figure 5. Temperature dependence of the ac susceptibility for $Nd_{0.75}Sr_{1.25}CoO_4$. ((a), (b)) The in-phase $\chi'(T)$ and out-of-phase $\chi''(T)$ components with a driving field of 1000 Oe at different frequency, 10, 200, and 1000 Hz. ((c), (d)) The in-phase $\chi'(T)$ and out-of-phase $\chi''(T)$ components with a frequency of 80 Hz at different driving field, 700, 1200, and 2000 Oe. The arrows in (b) and the inset note the x-coordinate positions of the peaks.

independent of temperature. Second, both signals compete with each other seriously between T_C and T_G. But, for PM states ($T \geqslant 220$ K) or FM states ($T \leqslant 150$ K), the ESR signals change very little.

Because the anomalous phenomena of dc magnetization and ESR spectra emerge in nearly the same temperature range as the materials that have a uniform structure, $La_{1-x}Sr_{1+x}MnO_4$ [3] and $(La, Sr)_2NiO_4$ [7], one may assume that all of them would originate from the same mechanism, i.e. charge ordering. However, in this way, the ferromagnetic correlation above

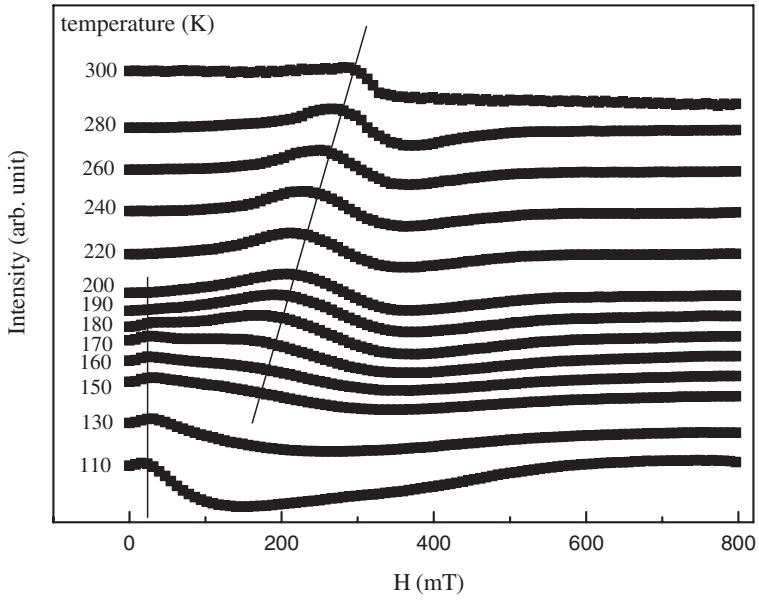

Figure 6. ESR spectra of $Nd_{0.75}Sr_{1.25}CoO_4$ at different temperature. The straight lines are guide to the eyes of the spectral evolution.

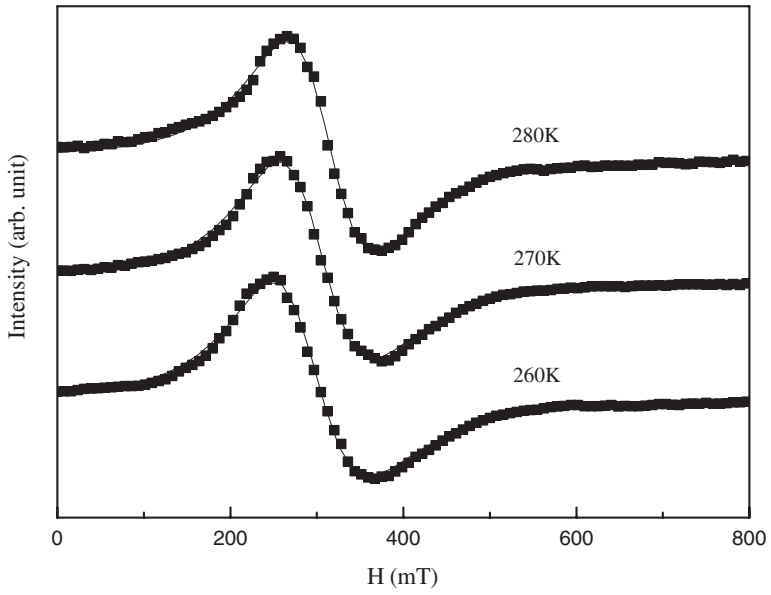

Figure 7. Line fits of the ESR spectra with Dysonian function at a few typical temperatures. The solid circles are the experimental data points and the smooth lines are the fits to Dysonian equation.

T_c should be quenched and the magnetization value should also be decreased below the charge-ordering temperature while the experimental magnetization increases. Recalling the theory proposed by Griffiths *et al*, the competition between the PM and FM signals and the anomaly in dc magnetization might show the existence of Griffiths singularities, i.e. the formation of

FM clusters in the PM background induces a deviation of $\chi(T)$ from the Curie–Weiss form, as seen in figures 2 and 3, and the FM clusters within the PM matrix lead to the magnetic heterogeneity, resulting in the anomalous paramagnetic behaviour in figures 4(b) and 6. Thus, T_G might be called the Griffiths temperature and the temperature range $T_C \leqslant T \leqslant T_G$ could be treated as the Griffiths phase for the material.

It is worthwhile to compare the magnetic properties of cobalt oxides with the analogous layered structure. Experiments on Sr_2CoO_4 revealed monotonous FM behaviour in the lower temperature range and PM behaviour in the higher temperature range [18]. But, for $La_{2-x}Sr_xCoO_4$ [3, 24], experiments revealed PM behaviour when $x \leqslant 1.1$ and FM behaviour when $x \geqslant 1.2$. The specimen also shows the spin-glass state (at ~20 K for $x = 0.4$ and 0.6, and ~8 K for $1.0 \leqslant x \leqslant 1.3$) and Griffiths singularities ($T_G \sim 200$ K for $1.0 \leqslant x \leqslant 1.5$), which is remarkably similar to that of $Nd_{0.75}Sr_{1.25}CoO_4$ in all respects except for the difference in the temperature point. Therefore, the anomalous magnetic properties of the layered cobalt oxides $Ln_{0.75}Sr_{1.25}CoO_4$ (Ln = La, Nd) may be due to the introduction of rare-earth ions, Ln^{3+}. That is, the substitution of Sr^{2+} by Ln^{3+} in the parent compound Sr_2CoO_4 induces cobalt ions with different valences and spins, Co^{3+} and Co^{4+}. The magnetic state is under competition between FM double-exchange interactions between Co^{3+} and Co^{4+} ions and the AFM super-exchange interactions between like ions. Moreover, the radii of the rare-earth ions are much smaller than that of the alkaline earth ion, $r_{Nd^{3+}}$(99.5 pm) $<$ $r_{La^{3+}}$(106.1 pm) $<$ $r_{Sr^{2+}}$(112 pm); the substitution of Sr^{2+} by Ln^{3+} would induce disorder in the quasi-two-dimensional structure. At temperatures below T_{SG}, the frustration of random competing interactions between FM and AFM results in spin-glass states. Also, at relatively high temperatures, the quenched disorder may contribute to the formation of the Griffiths-type phase. In contrast to the La^{3+} ion, the smaller size of the Nd^{3+} ion would enhance the effect of disorder that induces the higher T_{SG} and T_G. However, another layered cobalt oxide doped with rare-earth elements, $Sr_{2-x}Y_xCoO_4$, behaves without any trace of Griffiths singularities or spin-glass state but just the FM property, like Sr_2CoO_4, in the doping range $x \leqslant 0.5$ [17]. Also, the FM property disappears for $x \geqslant 0.67$. In this specimen, the size of Y^{3+} (90 pm) is much smaller than that of Nd^{3+}, which would seriously distort the lattice, as can be seen from the lattice parameters and bond lengths in the CoO_6 octahedron [13, 17]. Thus, the difference in the magnetic properties might be due to the size effect of Y^{3+}, which induces strong disorder. This case needs to be further investigated in the layered system with different rare-earth element doping.

In conclusion, the layered cobalt oxide $Nd_{0.75}Sr_{1.25}CoO_4$ undergoes PM states above 230 K, Griffiths phases between 230 and 179 K, FM states below 179 K, and spin-glass re-entry at around 18 K. The effective magnetic moment is 3.48 μ_B, suggesting that both Co^{3+} and Co^{4+} ions are in intermediate spin states above T_G. Comparing the magnetic properties of the analogous layered cobalt oxides, the Griffiths singularities and spin-glass states may be attributed to the introduction of rare-earth ions with a relatively small size, Nd^{3+}.

Acknowledgments

This work is supported by the Natural Science Foundation of China (nos. 10104013 & 50421201) and by the National Basic Research Program of China (no. 2006CB601003).

References

[1] Blasco J, Garcia J, Lazaro F J and Proietti M G 1995 *J. Magn. Magn. Mater.* **140–144** 1813
[2] Park J, Lee S and Park J-G 2000 *Phys. Rev.* B **62** 13848
[3] Moritomo Y, Higashi K, Matsuda K and Nakamura A 1997 *Phys. Rev.* B **55** R14725

[4] Ibrahim H M, Yassin O A, de Chatel P F and Bhatia S N 2005 *Solid State Commun.* **134** 695
[5] Deisenhofer J, Braak D, Krug von Nidda H-A, Hemberger J, Eremina R M, Ivanshin V A, Balbashov A M, Jug G, Loidl A, Kimura T and Tokura Y 2005 *Phys. Rev. Lett.* **95** 257202
[6] Rama N, Ramachandra Rao M S, Sankaranarayanan V, Majewski P, Gepraegs S, Opel M and Gross R 2004 *Phys. Rev.* B **70** 224424
[7] Griffiths R B 1969 *Phys. Rev. Lett.* **23** 17
[8] Bray A J 1987 *Phys. Rev. Lett.* **59** 586
[9] Salamon M B, Lin P and Chun S H 2002 *Phys. Rev. Lett.* **88** 197203
[10] Salamon M B and Chun S H 2003 *Phys. Rev.* B **68** 014411
[11] Li J Q and Yuan S L 2005 *Solid State Commun.* **134** 295
[12] Rama N, Opel M, Sankaranarayanan V, Gross R, Ogale S B, Venkatesan T and Ramachandra Rao M S 2005 *J. Appl. Phys.* **97** 10H713
[13] Sanchez-Andujar M and Senaris-Rodriguez M A 2004 *Solid State Sci.* **6** 21
[14] Castro-Garcia S, Sanchez-Andujar M, Rey-Cabezudo C, Senaris-Rodriguez M A and Julien C 2001 *J. Alloys Compounds* **323/324** 710
[15] Grandjean D and Weller M T 1993 *Mater. Res. Bull.* **28** 685
[16] Kittel C 1997 *Introduction to Solid State Physics* 7th edn (New York: Wiley)
[17] Wang X L and Takayama-Muromachi E 2005 *Phys. Rev.* B **72** 064401
[18] Matsuno J, Okimoto Y, Fang Z, Yu X Z, Matsui Y, Nagaosa N, Kawasaki M and Tokura Y 2004 *Phys. Rev. Lett.* **93** 167202
[19] Mydosh J A 1993 *Spin Glasses: An Experimental Introduction* (London: Taylor and Francis)
[20] Ivanshin V A, Deisenhofer J, Krug von Nidda H-A, Loidl A, Mukhin A A, Balbashov A M and Eremin M V 2000 *Phys. Rev.* B **61** 6213
[21] Joshi J P, Sood A K, Bhat S V, Parashar S, Raju A R and Rao C N R 2004 *J. Magn. Magn. Mater.* **279** 91
[22] Rettori C, Rao D, Singley J, Kidwell D, Oseroff S B, Causa M T, Neumeier J J, McClellan K J, Cheong S-W and Schultz S 1997 *Phys. Rev.* B **55** 3083
[23] Simon F, Atsarkin V A, Demidov V V, Gaal R, Moritomo Y, Miljak M, Janossy A and Forro L 2003 *Phys. Rev.* B **67** 224433
[24] Shimada Y, Miyasaka S, Kumai R and Tokura Y 2006 *Phys. Rev.* B **73** 134424